Protective function of autophagy during VLCFA-induced cytotoxicity in a neurodegenerative cell model

Margaux Doria, Thomas Nury, Dominique Delmas, Thibault Moreau, Gérard Lizard, Anne Vejux

Protective function of autophagy during VLCFA-induced cytotoxicity in a neurodegenerative cell model

Margaux Doria[1,2], Thomas Nury[1,2], Dominique Delmas[1,3], Thibault Moreau[1,2,4], Gérard Lizard[1,2], Anne Vejux[1,2]

1 – Université de Bourgogne Franche-Comté, Dijon, F-21000, France

2 - Team 'Biochemistry of the Peroxisome, Inflammation and Lipid Metabolism' EA 7270, Inserm, F-21000 Dijon, France

3 - Inserm Research Center LNC UMR U1231 - Team "Cancer and Adaptive Immune Response", Bioactive Molecules and Health research group, Dijon, F-21000, France

4 - Department of Neurology, University Hospital, F-21000 Dijon, France

E-mail addresses

M Doria: margaux.doria@hotmail.fr ;T. Nury: thomas.nury@u-bourgogne.fr, D. Delmas: dominique.delmas@u-bourgogne.fr, T. Moreau: thibault.moreau@chu-dijon.fr, G. Lizard: gerard.lizard@u-bourgogne.fr, A.Vejux: anne.vejux@u-bourgogne.fr

Correspondence:

Dr Anne Vejux, Université. Bourgogne Franche-Comté / Equipe Bio-PeroxIL (EA7270), UFR Sciences Vie Terre et Environnement, 6 Bd Gabriel, 21000 Dijon, France; Phone: +33 380 39 37 01; Fax: +33 380 39 62 50; Email: Anne.Vejux@u-bourgogne.fr

Abstract

In recent years, a particular interest has focused on the accumulation of fatty acids with very long chains (VLCFA) in the occurrence of neurodegenerative diseases such as Alzheimer's disease, multiple sclerosis or dementia. Indeed, it seems increasingly clear that this accumulation of VLCFA in the central nervous system is accompanied by a progressive demyelination resulting in death of neuronal cells. Nevertheless, molecular mechanisms by which VLCFA result in toxicity remain unclear. This study highlights for the first time in 3 different cellular models (oligodendrocytes 158N, primary mouse brain culture, and patient fibroblasts) the types of cell death involved where VLCFA-induced ROS production leads to autophagy. The autophagic process protects the cell from this VLCFA-induced toxicity. ~~Very interestingly, an omega 3, DHA, is able to inhibit this toxicity~~. Thus, autophagy in addition to oxidative stress can offer new therapeutic approaches.

Keywords : very long chain fatty acid, autophagy, lipotoxicity, neurodegenerative diseases, oxidative stress, ~~DHA,~~ rapamycin

Introduction

Many studies tend to demonstrate the role of exogenous and endogenous factors in brain aging, especially in patients with neurodegenerative diseases. Among these factors, some fatty acids with very long chains ($C \geq 22$) found at abnormally high concentrations seem to induce a significant toxicity in the central nervous system. This results in major dysfunctions that are found in many neurodegenerative pathologies and genetic diseases. For example, C22:0 (docosanoic acid or behenic acid) and very long-chain fatty acids (VLCFA, C24:0 (tetracosanoic acid or lignoceric acid) and C26:0 (hexacosanoic acid or cerotic acid)) accumulation was observed in patients with Alzheimer's disease (AD) with stage V-VI suggesting that peroxisome-related alterations in AD, through a VLCFA increase, may contribute to the progression of AD pathology [1]. Significant higher levels of C26:0 were also found in the plasma and red blood cells of patients with dementia [2]. In multiple sclerosis (MS), elevations in C26:0 were also found in MS grey matter [3]. Increased VLCFA levels were also found in the serum of MS patients [4]. Degradation of VLCFA by β-oxidation exclusively occurs in the peroxisome. In MS, this VLCFA accumulation implies the peroxisome: changes in the expression of the peroxisomal genes but also to the modification of the functionality of the peroxisomal proteins [3]. The neurodegenerative disease where the peroxisome was the most studied was X-linked adrenoleukodystrophy (X-ALD). X-ALD (OMIM 300100) is a rare genetic neurodegenerative disease and the most common and frequent peroxisomal disease. The X-ALD primarily affects male children at a rate of 1/17 000 births. Several molecular dysfunctions can contribute to VLCFA accumulation; this is mainly a decrease in peroxisomal β-oxidation and an increase in the elongation of fatty acids [5]. Others mechanisms may also contribute to this accumulation through genetic mutations such as the mutations in the gene ABCD1 (Xq28), encoding a peroxisomal member of the ATP-binding cassette (ABC) transporter subfamily D: ALDP ("AdrenoLeucoDystrophy

Protein") or ABCD1 [6, 7]. This transporter participates in the entry of VLCFA-CoA into the peroxisome. The mutations in gene ABCD1 cause loss expression or non-expression of functional protein leading to accumulation of VLCFA, mainly C24:0, C26:0 and C26:1, in tissue and plasma. This disease is also associated with progressive demyelination within the peripheral (PNS) and central nervous system (CNS), adrenal insufficiency and inflammatory process in areas of demyelination. In CNS, one of the cause of the demyelination process may be due to a loss of oligodendrocytes that are responsible for the synthesis of myelin sheaths, which enwrap axonal segments. These myelin alteration phenomena are present in demyelinating diseases such as MS and X-ALD. The most suitable study model is to use a line of oligodendrocytes, since these are the cells involved in the synthesis of myelin. A better understanding of interconnections between accumulation of VLCFA (due to peroxisome dysfunction) and oligodendrocyte cell death is still needed because these cells thus play a central role in the demyelination process. VLCFA could induce some types of cell death such as apoptosis, necrosis ([8] [9]). Nevertheless, the mechanisms are not well described and understand. Indeed, other types of death may involve the lysosomes that participate in the process of autophagy. The main objective is to determine whether apoptosis or necrosis are major phenomena involved in the death of oligodendrocyte cells involved in demyelination phenomena or whether there is another process involved such as autophagy. Our results have shown that following the accumulation of VLCFA, there is a production of ROS accompanied by an autophagic process. This process is a protective process for the accumulation of VLCFA, which leads to apoptosis and / or necrosis when it can no longer protect the cells.

Material and methods

Cell culture

Murine oligodendrocytes cells (158N) were seeded at 5,000–10,000 cells/cm^2 either in Petri dishes (100 mm in diameter), or 12-well plates, and cultured in Dulbecco's Modified Eagle Medium (DMEM) supplemented with 5% (v/v) heat-inactivated fetal bovine serum and 1% antibiotics (penicillin, streptomycin). The cells were incubated at 37°C in a humidified atmosphere containing 5% CO_2, trypsinized (0.05% trypsin-0.02% EDTA solution), and passaged twice a week. Human skin X-ALD fibroblasts (Coriell Institute GM17819) and WT human skin fibroblasts (Coriell Institute GM03348) were seeded at 7,500 cells/cm^2 and grown in Dulbecco's modified Eagle's medium supplemented with 10% fetal bovine serum at 37 °C under 5% CO_2 in the absence of antibiotics. The cells were passaged twice a week.

Mixed primary cultures of murine astrocytes and oligodendrocytes were isolated from one to three-days-old neonatal BALB/cJRj mice pups (Janvier-Europe), which were quickly beheaded. The brains were removed, placed in a Petri dish containing 10 mL DMEM medium, then meninges and blood vessels were removed by rolling on a sterilized filter paper. The cleaned brains were then placed in Petri dish containing 10 mL of complete medium (DMEM/10% FCS/1% antibiotics). Brain tissue, after gently diced into small pieces, has been dissociated mechanically on a 100 µm cellular sieve. Cells were harvested in 10 mL of complete medium, which were used to seed one 12 wells plate (800 µL/well). Primary cultures were incubated at 37°C in a humidified environment with 5% CO_2. After 4 days of culture, the medium was renewed, and then changed twice a week. After 10 days of culture, different treatments were realized.

Cell treatments

C24:0 (tetracosanoic acid) and C26:0 (hexacosanoic acid) were from Sigma–Aldrich (St. Louis, MO, USA). They were solubilized in α-cyclodextrin (Sigma–Aldrich) as previously described [10]. Final concentration of α-cyclodextrin (vehicle) in the culture medium is 1 mg/mL for the highest concentration used in VLCFA [11]. The cells were further treated for 6 h, 14 h, 24 h and/or 48 h with various VLCFA concentrations (1, 5, 10, and 20 µM) and with α-cyclodextrin (50 µM, 0.25 mM, 0.5 mM and 1 mM) in HAM's-F10 medium (medium containing no long chain fatty acid).

7-ketocholesterol (7KC, used as positive control) was provided by Sigma (L'Isle d'Abeau Chesnes, France). The purity of 7KC was determined to be 100% by gaseous phase chromatography coupled with mass spectrometry. For all experiments, a stock solution of 7KC was prepared at a concentration of 800 µg/mL, as previously described [12]. In all experiments, 7KC was added to the culture medium at the beginning of culture at a final concentration of 20 µg/mL, and treatments were carried out for 24 h.

Rapamycin was used as an inducer of autophagy (mTOR inhibitor that inhibits itself autophagy) and was provided by Sigma (L'Isle d'Abeau Chesnes, France). A stock solution was prepared at 1 mM in DMSO and stored at – 20°C. In all experiments, rapamycin was added to the culture medium at the beginning of culture at a final concentration of 5 µM with or without VLCFA (versus DMSO alone). Bafilomycin was used as an inhibitor of autophagy (inhibition of fusion between the lysosome and autophagosome, blocks the autophagic flux). A stock solution was prepared at 400 µM in DMSO and stored at – 20°C. In all experiments, bafilomycin was added to the culture medium 4 h before the end of culture at a final concentration of 400 nM (versus DMSO alone) with or without VLCFA.

3-methyladenin was prepared at 100 mM after light heating in water and used at 7.5 mM.

~~Docosahexaenoïc acid (DHA) was prepared at 8 mM in α-cyclodextrin (20 mM), conserved at 4°C and added in the culture medium at 50 µM with or without VLCFA~~.

Analysis of cell morphology by phase contrast microscopy

Cell morphology was observed after 24 h and 48 h of treatment in the absence or presence of VLCFA (1, 5, 10 and 20 µM), 7KC (20 µg/mL) and α-cyclodextrin under an inverted-phase contrast microscope (Axiovert 40CFL, Zeiss, Jena, Germany). Digitized images were obtained with a camera (Axiocam ICm1, Zeiss).

Colorimetric MTT assay

MTT assay was carried out on oligodendrocytes and fibroblasts plated in 48-wells flat bottom culture plates after 24 h or 48 h of treatment with C24:0 or C26:0 (1, 5, 10, and 20 µM) or 7KC (20 µg/mL) as previously described. The MTT assay was used to evaluate the effects of C24:0 and C26:0 on cell proliferation and/or viability. MTT salt is reduced to formazan in the metabolic active cells by dehydrogenase to form NADH and NADPH [13]. The plates were read at 570 nm with a microplate reader.

LDH Assay

Upon cell damage or lysis, lactate dehydrogenase (soluble enzyme located in the cytosol) is released in culture medium and can be considered as a measurement of cytotoxicity. In LDH cytotoxicity assay kit (Interchim), a coupled two-step reaction was used: 1) the reduction catalyzed by LDH of NAD^+ to NADH and H^+ by oxidation of lactate to pyruvate, 2) the newly-formed NADH and H+ was used by diaphorase to catalyze the reduction of a tetrazolium salt to colored formazan (490-520 nm). For the assay of released LDH, 100 µL of the cell supernatants was combined with 100 µL of reaction solution

containing NAD^+, lactic acid, tetrazolium salt, and diaphorase. LDH standards were used: 25 µL of LDH standard were added in the first tube with 475 µL de culture medium to obtain a concentration of 10 mU/mL (1 unit corresponds to the amount of LDH that catalyzes the reaction of 1 µmol of substrate per minute) and then doubling dilutions are realized in culture medium. Absorbance at 490 nm was measured after 1 h of incubation with gentle shaking at room temperature.

Flow cytometric measurement of cell viability with propidium iodide

Cell viability was determined with propidium iodide (PI; λEx_{max} = 540 nm, λEm_{max} = 625 nm, Sigma) (1 µg/ml) which binds to DNA by intercalating between the bases only if the plasma membrane is damaged as is the case for the dead cells [14]. The red fluorescence was quantified by flow cytometry in 10,000 cells on a logarithmic scale of fluorescence with a Galaxy flow cytometer (Partec-Sysmex). Fluorescence of PI was acquired by using a 630 nm longpass filter. Data were analyzed with FlowMax software (Partec-Sysmex).

Flow cytometric measurement of mitochondrial transmembrane potential with $DiOC_6(3)$

The mitochondrial transmembrane potential was measured by flow cytometry with 3,3'-dihexyloacarbocyanine iodide ($DiOC_6(3)$; λEx_{max} = 484 nm, λEm_{max} = 501 nm; Molecular Probes, Eugene, OR, USA) used at a final concentration of 40 nM. Flow cytometric analyses were performed with a Galaxy flow cytometer (Partec-Sysmex). The green fluorescence of $DiOC_6(3)$ was acquired with a 520/20 nm band pass filter and measured on a logarithmic scale. Data were analyzed with FlowMax software (Partec-Sysmex).

Flow cytometric measurement of reactive oxygen species production with dihydroethydium and 2',7'-dichlorofluorescein diacetate

Overproduction of superoxide anion ($O_2^{\bullet -}$) and reactive oxygen species including hydrogen peroxide, hydroxyl radicals and peroxynitrite, was detected with dihydroethidium (DHE; λEx_{max} = 518 nm, λEm_{max} = 605 nm, Life Technologies, St Aubin, France) and 2′,7′-dichlorofluorescein diacetate (H_2DCFDA, λEx_{max} = 495 nm, λEm_{max} = 527 nm, Life Technologies, St Aubin, France), respectively. DHE diffuses through cell membranes, and is rapidly oxidized into ethidium under the action of reactive oxygen species, mainly $O_2^{\bullet -}$. DHE (1.6 mM), prepared in dimethyl sulfoxide, was used at 2 µM. H_2DCFDA, cell-permeant compound, passively diffuses into cells and upon cleavage groups intracellular esterases and acetates by oxidation, the non-fluorescent H_2DCFDA dichlorofluorescein is converted to 2 ', 7' (DCF) highly fluorescent. After 15 min at 37°C, the fluorescent signals of DHE and H_2DCFDA stained cells were collected through a 590/10 nm and a 520/20 band pass filter, respectively, on a logarithmic scale on a GALAXY flow cytometer (Partec); 10,000 cells were acquired; data were analyzed with Flomax (Partec) software.

Measurement of catalase and superoxide dismutase activities

The measurement of catalase activity is based on the transformation of hydrogen peroxide in H_2O and dioxygen. More catalase activity will be higher; more hydrogen peroxide will be degraded. Cells washed in PBS were lysed in a RIPA buffer (10 mM Tris-HCl, pH 7.2, 150 mM NaCl, 0.5% Nonidet NP40, 0.5% Na deoxycholate, 0.1% SDS, 2 mM EDTA and 50 mM NaF) in the presence of 1/25 complete protease inhibitor cocktail tablets (Roche Diagnostics, Indianapolis, IN, USA) for 20 min on ice. Cell lysates were cleared by 15 min centrifugation at 12,000 g. The protein concentration was measured in the supernatant using the Bicinchoninic Acid Kit for Protein Determination (Sigma Aldrich). For the catalase activity measurement, a Mix containing Tris-HCl, pH 7.4, 1 M; H_2O_2, 400 mM; H_2O with a ratio

1/1/17 was prepared. 10 µL of protein lysate was added to 190 µL of Mix and the absorbance of H_2O_2 was measured at 240 nm using a Tecan Infinite 200Pro (Tecan, Lyon, France).

The superoxide dismutase (SOD) catalyzes the conversion of superoxide anions into hydrogen peroxide and dioxygen. SOD activity was measured with "SOD assay kit-WST" (Interchim). Cells, washed in PBS, were subjected to two freeze / thaw cycles then centrifuged at 10 000 g, 4°C. 20 µL of supernatant were added to reactional mix and incubated during 20 min at 37°C. The absorbance was measured at 450 nm using a Tecan Sunrise™ Reader (Tecan, Lyon, France).

Transmission electron microscopy

Transmission electron microscopy is a valuable tool for characterizing cell death. It was used to visualize the potential ultrastructural modifications induced by VLCFA (C24:0 and C26:0 10 or 20 µM; 24 h), a-cyclodextrin (1 mg/mL for 24 h, used as vehicle to dissolve VLCFA) and 7KC (20 µg/mL) on 158N cells, and was conducted as previously described [15].

Staining conditions with Monodansylcadaverine (MDC)

Staining with MDC (lysosomotropic agent and solvent polarity probe) has been described as identifying acidic compartments as autophagic vacuoles [16]. Its amino group can become protonated at low pH, leading to an ion trapping mechanism [17, 18]. MDC (λEx_{max} = 340 nm, λEm_{max} = 530 nm, Sigma) was prepared at 0,1 M in DMSO. Cells were seeded at 10 000 cells/cm^2 on 12-mm glass coverslips. After treatment, MDC was added to the culture medium at a final concentration of 0,005 mM. After 15 min of incubation at 37°C, cells were washed with PBS 1X. Slides were mounted in Dako fluorescent mounting medium (Dako), observations were made with an Axioskop microscope (Zeiss), and digitalized images were obtained with an Axiocam Zeiss camera.

Labeling of lysosomal compartment with LysoTracker

The characteristics and the cellular distribution of lysosomes, which can be evaluated using LysoTracker, was determined on 158N cells cultured on glass coverslips by staining with LysoTracker Red (Invitrogen) used at 1 mM. After labeling, the coverslips were washed in PBS, mounted in Dako fluorescent mounting medium (Dako), and observed under blue light. Observations were made under an Axioskop fluorescent microscope (Zeiss) using green excitation, and digitalized images were obtained with an Axiocam Zeiss camera.

Identification of LAMP1 by immunostaining

Cells were seeded at 10 000 cells/cm^2 on 12-mm glass coverslips. After treatment, cells were fixed with 4% paraformaldehyde (5–15 min; room temperature), washed three times with PBS, and incubated with blocking buffer (PBS, 0.05% saponine (Sigma–Aldrich), 10% goat or bovine serum (PANTM Biotech GmbH) (20 min; room temperature)). After washing in blocking buffer, cells were incubated (1 h; room temperature) with an anti-LAMP1 primary rabbit polyclonal antibody (Abcam) used at 1/300 (diluted in blocking buffer), washed twice in PBS, and then incubated for 30 min with a 594-Alexa goat anti-rabbit (Invitrogen) used at 1/300, respectively. Nuclei were counterstained with Hoechst 33342 (Sigma–Aldrich) used at 1 mg/mL. After washing with PBS, slides were mounted, observations were made with an Axioskop Zeiss microscope, and digitalized images were obtained with an Axiocam Zeiss camera.

Protein analysis by polyacrylamide gel electrophoresis and Western blotting

Cells were lysed in a lysis buffer (120 mM Tris-HCl, pH 6.8, 1, 4 % SDS) in the presence of 1/25 complete protease inhibitor cocktail tablets (Roche Diagnostics Corporation,

Indianapolis, IN, USA) for 30 min on ice. Cell lysates were cleared by a 15 min centrifugation at 20,000 *g*. The protein concentration was measured in the supernatant using the Bicinchoninic Acid Solution (Sigma-Aldrich). Fifty to eighty micrograms of proteins were diluted in loading buffer (20% glycerol, and 0.02% bromophenol blue), separated on a polyacrylamide SDS-containing gel, and transferred onto a nitrocellulose membrane (Thermo-Scientific, Waltham, MA, USA). After blocking nonspecific binding sites for 1h with 5% nonfat milk in TBST (10 mM Tris-HCl, 150 mM NaCl, 0.1% Tween 20, pH 8), the membrane was incubated overnight with the primary antibody diluted in TBST with 1-5% milk. The antibodies directed against active caspase-3 (#9662), and LC3-I/II (L8918) were from Cell Signaling (Ozyme, Saint Quentin Yvelines, France), and (Sigma-Aldrich), respectively, and used at 1/1000 final concentration. Antibody directed against β-actin (Sigma-Aldrich) was used at 1/10 000 final concentration. The membrane was then washed with TBST and incubated (1h, room temperature) with horseradish peroxidase-conjugated goat anti-mouse (Santa-Cruz Biotechnology) or anti-rabbit antibody (Santa-Cruz Biotechnology or Cell Signaling) diluted at 1/5 000. The membrane was washed with TBST and revealed using an enhanced chemiluminescence detection kit (Supersignal West Femto Maximum Sensitivity Substrate, Thermo-Scientific) and Chemidoc XRS+ (Bio-Rad). The level of cleaved caspase-3 was determined versus actin, and the ratio LC3-II/LC3-I was calculated with Image Lab software (Bio-Rad).

Results

VLCFA (C24:0 and C26:0) induce cell death of oligodendrocytes 158N cells

The effects of C24:0 and C26:0 were investigated at 1, 5, 10, and 20 µM on cell growth and viability of subconfluent 158N murine oligodendrocytes after 6, 14, 24 and 48 h of treatment. The concentrations were chosen according to the measurements made from the plasma of healthy subjects (1-5 µM) and patients with X-ALD (10-100 µM) and according to those frequently used in different *in vitro* and *in vivo* models of X-ALD (fibroblasts, 158N cells, rat hippocampal cell cultures of oligodendrocytes and astrocytes) [11, 19, 20]**.** Different tests were used to evaluate the effects of VLCFA on the 158N: MTT assay (based on succinate dehydrogenase activity, reflects cell proliferation and/or viability), propidium iodide (PI) staining for the identification of cells with damage plasma membrane and/or dead cells, release of LDH in the culture medium. Regardless of the considered test, the most pronounced effects were observed with C24: 0 and C26: 0 at 20 µM. The different results obtained are: 1) a reduction of MTT positive cells (Fig 1A, left), 2) a time dependent increase in the number of PI positive cells (Fig 1A, center), 3) a progressive increase in LDH release in the culture medium (Fig 1A, right). At 10 µM, the effects are less pronounced and are mainly observed with the MTT assay. VLCFA, at 1 or 5 µM, have no effect on cell viability. We observed the same effect in phase contrast microscopy (data not shown), over time and with increasing concentrations of VLCFA; the cells gradually take off from the culture dish. We can also notice that the 158N cells are somewhat more sensitive to C24:0 compared to C26:0. Together, these results show cytotoxic effects of VLCFA on oligodendrocyte 158N cells.

Apoptosis / necrosis pathways are not the primary events in the VLCFA-induced cell death

Using classical characterization methods of cell death, we evaluated the ability of VLCFA to induce necrosis or apoptosis, two major types of cell death, on 158N murine oligodendrocytes.

For these experiments, VLCFA were used at 10-20 µM after 6, 14, 24 and 48 h of treatment, which correspond to cytotoxic concentrations observed on 158N cells; 7-ketocholesterol (7KC; 20 µg/mL) was used as a positive compound of apoptosis as it is known to induce condensation/fragmentation of the nucleus and caspase-3 activation on U937 cells and 158N cells [21]. At 24 h of treatment with VLCFA, there were few cells (10%) positive with TUNEL staining (Supplementary data) and few cells (10%) with condensed/fragmented nuclei (Fig 1B). The activation of caspase-3 evaluated by the presence of cleaved capspase-3, was only observable for 24 h with the highest concentration in VLCFA: 20 µM (Supplementary data). In parallel, the percentage of cells with a necrotic profile (trypan blue positive cells) increased with time and with the concentration of VLCFA (Fig1B). Early necrosis sets in from 14h, with appearance of trypan blue colored cells but without correlation with LDH release, then necrosis is effective at 24h with a good correlation between the percentage of trypan blue colored cells and LDH release. Treatment with 7KC for 24 h induces an apoptotic mode of cell death: 95% of cells with condensed and/or fragmented nuclei characteristic of apoptotic cells; 65% of cells containing fragmented DNA (a late apptotic criteria) (Supplementary data). In addition, the use of a caspase inhibitor, z-vad-fmk, does not decrease the toxicity induced by VLCFA. Together, these results demonstrated that treatment with VLCFA do not induced apoptosis or necrosis of 158N cells before 24 h.

Reactive oxygen species production and antioxidant defences play a role in the effects of VLCFA (C24:0 and C26:0)

In neurodegenerative diseases such as Alzheimer's, Parkinson's disease or multiple sclerosis, the implication of oxidative stress ~~is no longer to be demonstrated~~ is well established. On the other hand, what is important in our model is to establish if an oxidative stress is well induced and what part is taken by this oxidative stress in the triggering of the death induced by the VLCFA.

Overproduction of superoxide anion ($O_2^{\bullet -}$) and reactive oxygen species that are key players in oxidative stress process was evaluated by DHE and H_2DCFDA, respectively, through a kinetic of 6 h to 48 h under treatment with VLCFA. The presence of superoxide anion was demonstrated at 24 h and 48 h with C24:0 and C26 0 (20 µM) (Fig. 2A). The increase in superoxide anion production was dependent on the duration of treatment. An increase in ROS levels in cells (increased oxidation of H_2DCFDA) was observed later to 48 h with VLCFA used at 20 µM (Fig. 2A).

Antioxidant defenses were evaluated by measuring catalase activity and superoxide dismutase activity. Catalase catalyzes the dismutation of hydrogen peroxide and superoxide dismutase allows the elimination of superoxide anions. VLCFA induced an increase in SOD activity at 14 h of treatment and this activity further decreases to the same level than in the control (Fig. 2B). VLCFA also induced an increase in catalase activity to 24 and / or 48 h of treatment according to the VLCFA considered and the concentration used (Fig. 2B). SOD activity is correlated with an increase in mitochondrial depolarization, which no longer allows mitochondrial SOD activity to be measured in late times (Fig. 2C).

Defense mechanisms would first be effective (no oxidative stress statistically detected at early times but a measure of SOD activity at 14 h.) and then these would be exceeded, resulting in significantly increased levels of ROS observed at 24 and 48 h. Treatment of oligodendrocytes

with VLCFA induces toxicity and oxidative stress at an early stage since activation of antioxidant defenses is measured at 14 h.

~~Are cell death observed by various authors is concomitant to this toxicity, or induced by it?~~

VLCFA (C24:0 and C26:0) induces relocation and aggregation of lysosomes in 158N cells

The physiopathology of different diseases is linked to the impaired function of the major cellular proteolytic mechanisms mediated especially by the lysosome. Indeed, the lysosomes can participate in the oxidative stress increases, the setting up of a cell death whether it is autophagic or not. In this way, we have tried to evaluate the involvement of lysosomes following treatment with VLCFA. Using transmission electron microscopy, it has been shown that vacuoles double membrane containing cellular compartments such as mitochondria, are present in the cytoplasm of C24:0- and C26:0-treated cells at VLCFA concentrations of 10 µM and compared with untreated cells or α-cyclodextrin-treated cells (Fig 3A). These vacuoles suggest the implication of lysosomes in the cell death induced by VLCFA (Fig 3A). Given the important position held by lysosomes in some process of vacuolisation, we evaluate the effects of VLCFA on lysosomal morphology, and cytoplasmic distribution of lysosomes on 158N cells treated with C24:0 and C26:0 at 5, 10, 20 µM for 6, 14, 24 and 48 h (Fig 3B). To determine these effects, observations were made using fluorescence microscopy with untreated, α-cyclodextrin-, or VLCFA-treated 158N cells cultured on glass slides and stained with LysoTracker or MDC, or immunolabelled with a LAMP1 rabbit polyclonal antibody. LysoTracker, that readily crosses cell membranes, is highly selective for acidic organelles, LAMP1 (Lysosomal-associated membrane protein 1) is considered as lysosome marker and MDC, lysosomotropic agent, preferentially accumulates in autophagic vacuoles. Under these conditions, when compared with untreated or α-cyclodextrin treated cells, topographical and

morphological changes are observed in lysosomes after LysoTracker staining or with LAMP1, mainly when VLCFA were used at 10 and 20 µM from 6 h treatment (Fig 3B). Thus, whereas the lysosomes were regularly distributed in the cytoplasm of untreated cells (or α-cyclodextrin-treated cells), relocation and aggregation of lysosomes are observed into the cytoplasm of the 158N cells treated by C24: 0 and C26: 0, mainly at 10 and 20 µM; there is also the presence of larger vacuoles (Fig 3B). In cells treated with C24:0 or C26:0 at 10 and 20 µM (24 h), 40 to 50 % of cells with changes in lysosome topography were observed. In untreated cells, MDC staining is uniform in the cytoplasm, whereas with treatment with VLCFA, wide green fluorescent structures are present in the cytoplasm. The percentage of cells, with these green fluorescent structures, was 30-35 % with C24:0 or C26:0 at 20 µM from 6 h of treatment. These different observations obtained with lysotracker and MDC staining, TEM and LAMP-1 immunolabelling suggest an implication of lysosomes in VLCFA-induced toxicity that could leading to an autophagic porcess. Indeed, during autophagic process, autophagosomes fuse with lysosomes, which induce the degradation of material sequestered.

Autophagy, a defense mechanism to protect oligodendrocytes from toxicities induced by VLCFA

During autophagy, the first step is autophagosome formation then fusion with lysosomes to form autolysosomes where there will be degradation of the material trapped in the double membrane vacuoles. To determine the induction of an autophagic process, we used LC3 (Light Chain 3) immunoblotting, bafilomycin A1 treatment and p62 immunolabelling. During elongation of autophagosome membrane, the LC3 protein is cleaved (LC3-I form) and conjugated to phosphatidylethanolamine (LC3-II form). The LC3-II form is built on both sides of the membrane of the autophagosome, and constitue a key marker of the formation of

autophagosome. In immunoblotting, we evaluate the effects of VLCFA on LC3 status on 158N cells treated with C24:0 and C26:0 at 1, 5, 10, and 20 µM for 6, 14, 24 and 48 h compared to the 7KC used at 50 µM (Fig 4A). 7-ketocholesterol is an inducer of autophagy on 158N cells, with an increase in the presence of the LC3-II form at 14 h of treatment. Concerning the VLCFA, the C24: 0 to 10 µM induces an increase in the LC3-II form from 24 h of treatment, to 20 µM an increase of the form LC3-II is observed from 14 h of treatment. For C26: 0, an increase of the LC3-II form is observed from 24 h of treatment (Fig 4A). The results obtained (increase in LC3-II) can be interpreted in two different ways: upregulation of autophagosome formation or blockage of autophagic degradation. In order to answer this question, inhibitors acting on the lysosomes can be used. Bafilomycin A1 was used as an inhibitor of late stages of autophagy, inhibiting fusion between lysosomes and autophagosomes. The results obtained with bafilomycin A1 will provide information on autophagic flux, and allow us to determine whether the autophagic process is inhibited or not. If the levels of LC3-II remain unchanged in the presence of inhibitor, this will mean that the observed increase without inhibitor is due to blocked autophagic flux. On the other hand, if the levels increase in the presence of inhibitor, this will indicate that there is an increase in the autophagic flux under the effect of the treatment. This is what we observe here, during treatment with VLCFA, there is an increase in the levels of LC3-II between the conditions without and with inhibitor (Bafilomycin A1) (Fig 4B). This indicates that the VLCFA induces an autophagic process which degrades the contents of the vacuoles by the lysosomes.

To confirm these results, we carry out an immunolabeling of the p62 protein. Protein p62 is involved in autophagic process and is degraded by autophagy; its presence in vacuoles and the size of these vacuoles were evaluated (Fig 4C). A marked increase in the number and size of p62 positive vacuoles, when cells are treated with VLCFAs, is observed, unlike untreated cells, where diffuse scarring in the cytoplasm is observed. At 6 h of treatment, with the

VLCFA at 20 µM, diffuse labeling is observed in the cytoplasm with the appearance of some positive p62 vacuoles (Fig 4C). At 6 h of treatment, for C24: 0 and C26: 0 to 10 µM, 10% and 22% of the cells possess positive p62 vacuoles respectively. While 80 and 75% of the cells possess vacuoles with C24: 0 and C26: 0 to 20 µM respectively. The longer the treatment time, more p62 positive vacuoles are observed. Thus at 24 h, more than 70% of the cells are p62 positive with C24: 0 to 10 and 20 µM, while 50% and 87% of the cells have positive p62 vacuoles with C26: 0 to 10 and 20 µM respectively (Fig 4C).

The VLCFA induce an autophagic process that appears early, without being inhibited during its development, going as far as the recycling of autolysosomes.

In order to investigate whether the autophagic process was responsible for the cell death of oligodendrocytes following the accumulation of VLCFAs, the inhibitor of the molecular target of rapamycin (mTOR), that plays a crucial role in regulating autophagy, rapamycin was used (when mTOR is inhibited, autophagy is activated). If using rapamycin, more cell death is observed, this will indicate that autophagy is involved in the VLCFA-induced cell death of oligodendrocytes. If, on the contrary, an increase in survival is observed, this will indicate that autophagy is a protective mechanism that is set up to respond to the toxicity induced by VLCFA. We place ourselves at 24 h and 48 h of treatment where the effects are most visible in terms of toxicity. The effects of rapamycin are evaluated by phase contrast microscopy (Fig 4D) and MTT (Fig 4D). When the cells are treated with C24: 0 or C26: 0 to 20 µM, there is a decrease in the number of cells and a rounding of the cells, compared to the control cells (Fig 4D). When a rapamycin co-treatment (5 µM) / VLCFA (20 µM) is used, an increase in the number of cells present and a larger spreading of the cells is observed (Fig 4D). Similar results are obtained with the MTT test. When cells are treated with VLCFA, mitochondrial activity and / or cell number decrease, while rapamycin is added, mitochondrial activity and / or cell number increase without a return to value of control (Fig 4D). The activation of

autophagy by the use of rapamycin protects the cells from the toxicity induced by the VLCFA. The involvement of autophagy as a protective mechanism is confirmed by the use of 3-methyladenine which is an inhibitor of the autophagic pathway. At a concentration of 7.5 mM, we obtained a decrease in the number of MTT positive cells, indicating an increase in VLCFA toxicity in the presence of an autophagy inhibitor (Supp Data 2).

Autophagy, observed following an accumulation of VLCFA, protects against the cytotoxicity induced by these same VLCFAs.

VLCFA-induced autophagy is reproduced in a mixed primary culture from mouse brain

In the nervous system, oligodendrocytes interact with neurons, and astrocytes. In a primary culture model of mouse brain, these different cell types can be found. In this mixed culture model, the majority cells are the astrocytes, and then the oligodendrocytes, some neurons are present. These mixed cultures were treated with VLCFA. Their effects were evaluated using an MTT test (evaluation of mitochondrial activity and / or number of cells), by studying the secretion of LDH in the culture medium, the presence of an apoptotic and / or autophagic process. At the level of toxicity analysis, as for 158N cells, VLCFAs induce a decrease in the number of live cells and / or the number of cells with functional mitochondria when using the MTT test (FIG. 5A). This decrease occurs in a dose-dependent manner. The toxic effect of VLCFA is observable from 6 hours of treatment with a reduction of nearly 50% of the reduction rate of MTT for the 10 µM concentration. The release of LDH into the culture medium is observable from 6 hours of treatment but at higher concentrations 20 µM (Fig 5B). With respect to the possible induction of apoptosis death, Hoechst 33342 staining was performed but no condensed and / or fragmented nuclei were found (data not shown). The effect of VLCFA on the induction of a possible autophagic process was evaluated, a decrease in the LC3-I form and an increase in the LC3-II form was observed when primary cultures

were treated with VLCFA (Fig. 5C). The presence of an autophagic process is mainly detected for concentrations at 20 µM for C24: 0 or C26: 0 at early treatment times from 10 h (Fig. 5C). This autophagic process takes place until the lysosomes degrade the contents of the vacuoles. Indeed, when the mixed cultures of cells are treated with bafilomycin A1 and the VLCFAs, an increase in the LC3-II / LC3-I ratio is observed (FIG. 5D). Immunolabelling of the p62 protein was also performed. The presence of p62 positive vacuoles is detected as early as 6 h of treatment, for the concentration at 20 µM (Fig 5E). VLCFAs are toxic at 20 µM on mixed cultures of cells, and induce a non-apoptotic death process associated with the induction of an autophagic process. The presence of cell types other than oligodendrocytes does not alter the sequence of events as they have been described with the 158N cell line.

X-ALD patient fibroblasts reflect the autophagy process induced by VLCFA

The results obtained previously were in a general context of neurodegenerative diseases where oligodendrocytes may be involved. The results obtained are therefore tested on an example of a neurodegenerative disease, X-ALD. To study the cytotoxicity on cells of the central nervous system, very few cellular models based on the use of cells from patients exists. The models available are models of skin fibroblasts obtained after biopsy. The effect of very long-chain fatty acids has been studied on WT fibroblasts (GM03348, Coriell Institute) and on X-ALD fibroblasts (GM17819, Coriell Institute), the latter no longer express the ABCD1 protein and have a β -oxidation greatly diminished. The fibroblasts were treated with C24: 0 and C26: 0 at concentrations of 10 and 20 µM for 6, 14, 24 and 48 h. Their effects were evaluated using an MTT assay (evaluation of mitochondrial activity and / or number of cells), and by studying the presence of an apoptotic and / or autophagic process. In these cells,

the decrease in MTT reduction is greater when VLCFA concentration and duration of treatment increase, however X-ALD fibroblasts appear to be more sensitive to VLCFA than WT fibroblasts (Fig 6A/B). At 24 h of treatment, the rate of reduction of MTT increases from 100% for non-treated cells to 60% for WT fibroblasts and to 50% for X-ALD fibroblasts when treated with C24: 0 to 20 μM. This difference is more marked with C26: 0 to 20 μM, with a reduction of MTT to 50% for WT fibroblasts and to 30% for X-ALD fibroblasts. With respect to the possible induction of apoptosis death, Hoechst 33342 staining was performed but no condensed and / or fragmented nuclei were found. The possible induction of a process of autophagy was evaluated by studying the cleavage and binding to phospholipids of the LC3 protein (Fig. 6B) and by immunolabelling the p62 protein (Fig 6D). In WT fibroblasts, there was no change in the LC3-II ratio on LC3-I during VLCFA treatments. On the other hand, in X-ALD fibroblasts, an increase in the LC3-II / LC3-I ratio depending on the treatment time and the VLCFA concentration is observed. At 24 h of treatment, this ratio is multiplied by two when X-ALD fibroblasts are treated with C24: 0 to 20 μM and multiplied by three when treated with C26: 0 to 20 μM (Fig 6B). When the mixed cultures of cells are treated with bafilomycin A1 and the VLCFAs, an increase in the LC3-II / LC3-I ratio is observed, indicating that the induced autophagic process continues to its full term i.e. the degradation of the vacuolar content (Fig 6C). Immunolabelling of the p62 protein was also performed. In WT or X-ALD fibroblasts, controls (untreated) or treated by the vehicle (α-cyclodextrin), diffuse scarring is observed in the cytoplasm. In the WT cells, some vacuoles are present. X-ALD fibroblasts exhibit larger and larger vacuoles. These different data suggest that when the cells are deficient in ABCD1 transporter and accumulate VLCFAs, there is induction of an autophagic process as could be shown with 158N oligodendrocytes and astrocyte / oligodendrocyte mixed primary cultures.

DISCUSSION

Age-related diseases, particularly neurodegenerative diseases, are becoming increasingly important in terms of public health. However, the mechanisms underlying these pathologies are still not well known. Many factors can be taken into account, such as metabolic factors with the accumulation of very long chain fatty acids due to a defect in the metabolism of peroxysomes. The various experiments conducted aim to improve the knowledge of how VLCFAs work by using an oligodendrocyte model, which are myelin synthesizing cells and are therefore key elements in demyelinating neurodegenerative diseases. The mechanisms identified were also assessed in the specific context of X-linked adrenoleukodystrophy. Indeed, X-linked adrenoleukodystrophy is the most frequent neurodegenerative peroxisomal disorder, caused by mutations in the *ABCD1* gene and characterized by VLCFA accumulation, abnormal myelination and cell death. A better knowledge of the mechanisms involved would make it possible to envisage new therapeutic approaches. Taking the example of X-ALD, current therapies are not yet fully satisfactory. Curative therapy for X-ALD patients is not available. Therapeutic strategies targeting VLCFA (Lorenzo's oil) have failed to stop cerebral involvements [22]. Allogenic bone marrow transplantation is an effective treatment but associated with morbidity and mortality. Another possibility is hematopoietic stem cell gene therapy which is effective, but with possibilities of use that seem restricted. It is therefore necessary to continue to seek potential therapeutic targets.

The various experiments previously carried out on the action of very long chain fatty acids and oligodendrocytes, in particular the work of Baarine et al, were carried out under conditions where the medium was either serum-free or with a small percentage of serum [23]. Since the percentage of serum is an important factor for cell growth and/or the induction of certain death processes such as autophagy, toxicity and oxidative stress studies were carried out under normal culture conditions, i. e. with 5% SVF but with a medium that does not

contain VLCFA. The results obtained are similar to those presented by Baarine et al [23]. We therefore went further in determining the mechanisms of cell death induced by VLCFAs in the oligodendrocyte model. One possibility is to prevent the cell death of the cells of the neuronal nervous system and more particularly that of the oligodendrocytes, cells that synthesize myelin. Different groups have studied cell death in the nervous system in the context of X-ALD but the type of death described is different. Death by necrosis or by apoptosis has been described. In the brain of X-ALD patients, apoptotic death (DNA ladder pattern and terminal deoxynucleotidyl transferase staining) was observed [24]. In the brain of patients suffering from the brain shape of X-ALD, oligodendrocytes die by apoptosis with evidence of activated caspase-3 and fragmentation of DNA [25]. Death by apoptosis has also been observed in brain areas with microglia activation [26]. The Ito group, on the other hand, described a death of the oligodendrocytes by cytolysis [9]. This study shows that there is certainly a process of apoptosis and loss of membrane integrity but these two processes occur at late times and are probably the consequence of impossibility for the cell to resist the damage induced by the accumulation of VLCFAs. These results may explain the discrepancies observed in the brains of patients of the studies cited above. On the other hand, what is interesting is that the cells respond to the accumulation of VLCFA by the induction of an autophagic process. This autophagic process is observed at early times and is accompanied by mitochondrial involvement and oxidative stress. These last two processes have already been demonstrated *in vivo* (organotypic culture of spinal cord) or *in vitro* (human fibroblasts), which validates our different models used [20]. Autophagy is a physiological process that allows the cell to respond to stress by recycling its own constituents but can become deleterious when the cell can no longer counteract stress. This leads to the activation of other cell death pathways such as apoptosis and necrosis [27]. In neurodegenerative diseases, autophagy is rather presented as a protective mechanism when induced. Whether in

neurodegenerative diseases or other pathologies, the mTOR protein is described as a potential target; we have therefore chosen to use rapamycin to evaluate the protective or deleterious effects of the autophagic process [28, 29]. It was demonstrated that the autophagic process induced to its full term ie the degradation of the material contained in the autophagolysosomes and that this process was rather a protector for the cells via the use of rapamycin. Indeed, in experiments with rapamycin, we were able to show that an induction of the autophagic process made it possible to reduce the toxicity induced by the very long chain fatty acids. Autophagy would be a protective mechanism put in place following the stress induced by the accumulation of VLCFA. In some cells, this protection would not be sufficient and would lead to the appearance of apoptotic or necrotic processes as we observed in later times. Launay et al showed in a mouse model X-ALD ($Abcd1^{-}$ / $Abcd2^{-/-}$) that when they used a derivative of rapamycin (tensirolimus), they restored autophagic flux and inhibited axonal degeneration [30]. In addition, the Smith team demonstrated that induction of autophagy decreased demyelination in a rat animal model possessing a mutation in the gene coding for the Myelin Basic Protein [31]. Autophagy can be a therapeutic target considered in addition to the existing therapies and described previously, since the use of dietary rapamycin may have been shown to be effective in other conditions such as age-related vascular dysfunctions [32]. Autophagy and neurodegenerative diseases are closely linked. In many neurodegenerative diseases, there is a malfunction of the autophagic process: impaired autophagosome formation (Alzheimer's, Parkinson's, Huntington's, Amyotrophic lateral sclerosis), disrupted lysosomal function (Alzheimer's, Parkinson's [33]. For these pathologies, research is oriented towards activators of autophagy of natural origin, which can lead to the development of new drugs, as in the case of Parkinson's disease : Oxindole alkaloids isolated from U. rhynchophylla, Conophylline, polyphenols (curcumin, resveratrol, Amurensin G), or disaccharides, triterpenes, flavonoids [34].

The results of this study are in favor of an intensive search for new molecules natural or not able to activate the autophagy at the neuronal level or reduce VLCFA toxicity at an early stage

Funding sources

This work was supported by grants from: Université de Bourgogne; "Association Bourguignonne pour les Applications des Sciences de l'Information en Médecine" (ABASIM, Dijon, France), Rotary-Club de Dijon Bourgogne (Club N° 11296), Bonus Qualité Recheche Bourgogne/Franche-Comté Funding, and Department of Neurology (University Hospital, Dijon, France)

References

[1] J. Kou, G.G. Kovacs, R. Hoftberger, W. Kulik, A. Brodde, S. Forss-Petter, S. Honigschnabl, A. Gleiss, B. Brugger, R. Wanders, W. Just, H. Budka, S. Jungwirth, P. Fischer, J. Berger, Peroxisomal alterations in Alzheimer's disease, Acta Neuropathol 122(3) (2011) 271-83.
[2] A. Zarrouk, J.M. Riedinger, S.H. Ahmed, S. Hammami, W. Chaabane, M. Debbabi, S. Ben Ammou, O. Rouaud, M. Frih, G. Lizard, M. Hammami, Fatty acid profiles in demented patients: identification of hexacosanoic acid (C26:0) as a blood lipid biomarker of dementia, J Alzheimers Dis 44(4) (2015) 1349-59.
[3] E. Gray, C. Rice, K. Hares, J. Redondo, K. Kemp, M. Williams, A. Brown, N. Scolding, A. Wilkins, Reductions in neuronal peroxisomes in multiple sclerosis grey matter, Mult Scler 20(6) (2014) 651-9.
[4] V.K. Senanayake, W. Jin, A. Mochizuki, B. Chitou, D.B. Goodenowe, Metabolic dysfunctions in multiple sclerosis: implications as to causation, early detection, and treatment, a case control study, BMC Neurol. 15 (2015) 154.
[5] M. Baarine, M. Khan, A. Singh, I. Singh, Functional Characterization of IPSC-Derived Brain Cells as a Model for X-Linked Adrenoleukodystrophy, PloS one 10(11) (2015) e0143238.
[6] J. Mosser, A.M. Douar, C.O. Sarde, P. Kioschis, R. Feil, H. Moser, A.M. Poustka, J.L. Mandel, P. Aubourg, Putative X-linked adrenoleukodystrophy gene shares unexpected homology with ABC transporters, Nature 361(6414) (1993) 726-30.
[7] F. Geillon, D. Trompier, C. Gondcaille, G. Lizard, S. Savary, [Peroxisomal ABC transporters and X-linked adrenoleukodystrophy], Medecine sciences : M/S 28(12) (2012) 1087-94.
[8] B. Ahlemeyer, M. Gottwald, E. Baumgart-Vogt, Deletion of a single allele of the Pex11beta gene is sufficient to cause oxidative stress, delayed differentiation and neuronal death in mouse brain, Dis Model Mech 5(1) (2012) 125-40.
[9] M. Ito, B.M. Blumberg, D.J. Mock, A.D. Goodman, A.B. Moser, H.W. Moser, K.D. Smith, J.M. Powers, Potential environmental and host participants in the early white matter lesion of adreno-

leukodystrophy: morphologic evidence for CD8 cytotoxic T cells, cytolysis of oligodendrocytes, and CD1-mediated lipid antigen presentation, J. Neuropathol. Exp. Neurol. 60(10) (2001) 1004-19.
[10] I. Singh, Y. Kishimoto, Effect of cyclodextrins on the solubilization of lignoceric acid, ceramide, and cerebroside, and on the enzymatic reactions involving these compounds, J. Lipid Res. 24(5) (1983) 662-5.
[11] S. Hein, P. Schonfeld, S. Kahlert, G. Reiser, Toxic effects of X-linked adrenoleukodystrophy-associated, very long chain fatty acids on glial cells and neurons from rat hippocampus in culture, Hum. Mol. Genet. 17(12) (2008) 1750-61.
[12] T. Nury, A. Zarrouk, A. Vejux, M. Doria, J.M. Riedinger, R. Delage-Mourroux, G. Lizard, Induction of oxiapoptophagy, a mixed mode of cell death associated with oxidative stress, apoptosis and autophagy, on 7-ketocholesterol-treated 158N murine oligodendrocytes: Impairment by alpha-tocopherol, Biochemical and biophysical research communications (2013).
[13] T. Mosmann, Rapid colorimetric assay for cellular growth and survival: application to proliferation and cytotoxicity assays, J. Immunol. Methods 65(1-2) (1983) 55-63.
[14] C.J. Yeh, B.L. Hsi, W.P. Faulk, Propidium iodide as a nuclear marker in immunofluorescence. II. Use with cellular identification and viability studies, J. Immunol. Methods 43(3) (1981) 269-75.
[15] K. Ragot, J.J. Mackrill, A. Zarrouk, T. Nury, V. Aires, A. Jacquin, A. Athias, J.P. Pais de Barros, A. Vejux, J.M. Riedinger, D. Delmas, G. Lizard, Absence of correlation between oxysterol accumulation in lipid raft microdomains, calcium increase, and apoptosis induction on 158N murine oligodendrocytes, Biochem Pharmacol 86(1) (2013) 67-79.
[16] A. Biederbick, H.F. Kern, H.P. Elsasser, Monodansylcadaverine (MDC) is a specific in vivo marker for autophagic vacuoles, Eur. J. Cell Biol. 66(1) (1995) 3-14.
[17] A. Niemann, J. Baltes, H.P. Elsasser, Fluorescence properties and staining behavior of monodansylpentane, a structural homologue of the lysosomotropic agent monodansylcadaverine, The journal of histochemistry and cytochemistry : official journal of the Histochemistry Society 49(2) (2001) 177-85.
[18] A. Niemann, A. Takatsuki, H.P. Elsasser, The lysosomotropic agent monodansylcadaverine also acts as a solvent polarity probe, The journal of histochemistry and cytochemistry : official journal of the Histochemistry Society 48(2) (2000) 251-8.
[19] J. Galino, M. Ruiz, S. Fourcade, A. Schluter, J. Lopez-Erauskin, C. Guilera, M. Jove, A. Naudi, E. Garcia-Arumi, A.L. Andreu, A.A. Starkov, R. Pamplona, I. Ferrer, M. Portero-Otin, A. Pujol, Oxidative damage compromises energy metabolism in the axonal degeneration mouse model of X-adrenoleukodystrophy, Antioxid. Redox Signal. 15(8) (2011) 2095-107.
[20] S. Fourcade, J. Lopez-Erauskin, J. Galino, C. Duval, A. Naudi, M. Jove, S. Kemp, F. Villarroya, I. Ferrer, R. Pamplona, M. Portero-Otin, A. Pujol, Early oxidative damage underlying neurodegeneration in X-adrenoleukodystrophy, Hum. Mol. Genet. 17(12) (2008) 1762-73.
[21] T. Nury, A. Zarrouk, J.J. Mackrill, M. Samadi, P. Durand, J.M. Riedinger, M. Doria, A. Vejux, E. Limagne, D. Delmas, M. Prost, T. Moreau, M. Hammami, R. Delage-Mourroux, N.M. O'Brien, G. Lizard, Induction of oxiapoptophagy on 158N murine oligodendrocytes treated by 7-ketocholesterol-, 7beta-hydroxycholesterol-, or 24(S)-hydroxycholesterol: Protective effects of alpha-tocopherol and docosahexaenoic acid (DHA; C22:6 n-3), Steroids 99(Pt B) (2015) 194-203.
[22] H.W. Moser, A.B. Moser, K. Hollandsworth, N.H. Brereton, G.V. Raymond, "Lorenzo's oil" therapy for X-linked adrenoleukodystrophy: rationale and current assessment of efficacy, J. Mol. Neurosci. 33(1) (2007) 105-13.
[23] M. Baarine, P. Andreoletti, A. Athias, T. Nury, A. Zarrouk, K. Ragot, A. Vejux, J.M. Riedinger, Z. Kattan, G. Bessede, D. Trompier, S. Savary, M. Cherkaoui-Malki, G. Lizard, Evidence of oxidative stress in very long chain fatty acid--treated oligodendrocytes and potentialization of ROS production using RNA interference-directed knockdown of ABCD1 and ACOX1 peroxisomal proteins, Neuroscience 213 (2012) 1-18.
[24] I. Singh, K. Pahan, M. Khan, A.K. Singh, Cytokine-mediated induction of ceramide production is redox-sensitive. Implications to proinflammatory cytokine-mediated apoptosis in demyelinating diseases, J. Biol. Chem. 273(32) (1998) 20354-62.

[25] V. Feigenbaum, A. Gelot, P. Casanova, C. Daumas-Duport, P. Aubourg, M. Dubois-Dalcq, Apoptosis in the central nervous system of cerebral adrenoleukodystrophy patients, Neurobiol Dis 7(6 Pt B) (2000) 600-12.
[26] F.S. Eichler, J.Q. Ren, M. Cossoy, A.M. Rietsch, S. Nagpal, A.B. Moser, M.P. Frosch, R.M. Ransohoff, Is microglial apoptosis an early pathogenic change in cerebral X-linked adrenoleukodystrophy?, Ann. Neurol. 63(6) (2008) 729-42.
[27] G. Kroemer, L. Galluzzi, P. Vandenabeele, J. Abrams, E.S. Alnemri, E.H. Baehrecke, M.V. Blagosklonny, W.S. El-Deiry, P. Golstein, D.R. Green, M. Hengartner, R.A. Knight, S. Kumar, S.A. Lipton, W. Malorni, G. Nunez, M.E. Peter, J. Tschopp, J. Yuan, M. Piacentini, B. Zhivotovsky, G. Melino, D. Nomenclature Committee on Cell, Classification of cell death: recommendations of the Nomenclature Committee on Cell Death 2009, Cell Death Differ. 16(1) (2009) 3-11.
[28] A. Kaur, S. Sharma, Mammalian target of rapamycin (mTOR) as a potential therapeutic target in various diseases, Inflammopharmacology 25(3) (2017) 293-312.
[29] D. Zemke, S. Azhar, A. Majid, The mTOR pathway as a potential target for the development of therapies against neurological disease, Drug News Perspect 20(8) (2007) 495-9.
[30] N. Launay, C. Aguado, S. Fourcade, M. Ruiz, L. Grau, J. Riera, C. Guilera, M. Giros, I. Ferrer, E. Knecht, A. Pujol, Autophagy induction halts axonal degeneration in a mouse model of X-adrenoleukodystrophy, Acta neuropathologica 129(3) (2015) 399-415.
[31] C.M. Smith, J.A. Mayer, I.D. Duncan, Autophagy promotes oligodendrocyte survival and function following dysmyelination in a long-lived myelin mutant, J. Neurosci. 33(18) (2013) 8088-100.
[32] L.A. Lesniewski, D.R. Seals, A.E. Walker, G.D. Henson, M.W. Blimline, D.W. Trott, G.C. Bosshardt, T.J. LaRocca, B.R. Lawson, M.C. Zigler, A.J. Donato, Dietary rapamycin supplementation reverses age-related vascular dysfunction and oxidative stress, while modulating nutrient-sensing, cell cycle, and senescence pathways, Aging Cell 16(1) (2017) 17-26.
[33] F.M. Menzies, A. Fleming, A. Caricasole, C.F. Bento, S.P. Andrews, A. Ashkenazi, J. Fullgrabe, A. Jackson, M. Jimenez Sanchez, C. Karabiyik, F. Licitra, A. Lopez Ramirez, M. Pavel, C. Puri, M. Renna, T. Ricketts, L. Schlotawa, M. Vicinanza, H. Won, Y. Zhu, J. Skidmore, D.C. Rubinsztein, Autophagy and Neurodegeneration: Pathogenic Mechanisms and Therapeutic Opportunities, Neuron 93(5) (2017) 1015-1034.
[34] Z.Y. Wang, J.Y. Liu, C.B. Yang, S. Malampati, Y.Y. Huang, M.X. Li, M. Li, J.X. Song, Neuroprotective Natural Products for the Treatment of Parkinson's Disease by Targeting the Autophagy-Lysosome Pathway: A Systematic Review, Phytother. Res. (2017).

Figure legends

Figure 1: Evaluation of cytotoxicity of VLCFA (C24:0 and C26:0) on 158N murine oligodendrocytes. 158N cells were cultured for 6, 14, 24 and 48 h in the absence or presence C24:0 and C26:0 in a range of concentrations from 1 to 20 µM. A: On the left grafts, the effects of VLCFA on cell proliferation and mitochondrial metabolism were evaluated with the MTT assay. The integrity of cytoplasmic membranes of cells was evaluated with the PI test presented on the charts at the center and with LDH assay on the right grafts. B: The percentage of apoptotic cells (cells with condensed and/or fragmented nuclei) was determined by fluorescence microscopy after staining with Hoechst 33342 (black bars) and the percentage of necrotic cell was determined with trypan blue (white bars). Data shown are mean ± SD from minimum three independent experiments realized in triplicat. Significance of the

difference between VLCFA-treated cells and α-cyclodextrin-treated cells was determined with Mann-Whitney test: * $p < 0.05$; ** $p<0.01$, *** $p<0.001$, and # $p<0.0001$.

Figure 2: Effects of VLCFA (C24:0 and C26:0) on ROS production and anti-oxidant defense mechanisms on 158N murine oligodendrocytes. Murine oligodendrocytes (158N) were cultured for 6, 14, 24 and 48 h in the absence (control) or in the presence of α-cyclodextrin (vehicle: 1 mM) or VLCFA (C24:0 or C26:0: 1, 5, 10, 20 µM). A: ROS production - The effects of C24:0 and C26:0 on the production of intracellular superoxide anion ($O_2^{\cdot -}$) and on the production of intracellular ROS production were evaluated with DHE and H_2DCFDA. B: Anti-oxidant defense mechanisms were evaluated with catalase activity and superoxide dismutase (SOD) activity. Data shown are mean ± SD from minimum three independent experiments realized in triplicat. Significance of the difference between VLCFA-treated cells and α-cyclodextrin-treated cells was determined with Mann-Whitney test: * $p < 0.05$; ** $p<0.01$, *** $p<0.001$, and # $p<0.0001$.

Figure 3: Effects of VLCFA (C24:0 and C26:0) on lysosomes on 158N murine oligodendrocytes. A: Ultrastuctural features of 158N murine oligodendrocytes treated with VLCFA. Subconfluent 158N cells were cultured without or with C24:0 and C26:0 at 20 µM. or with α-cyclodextrin (vehicle: 1 mM) for 24 h. B: Effects of C24:0 and C26:0 (10 and 20 mM; 6 and 24 h) on the morphological aspects and on the distribution of lysosomes evaluated by staining with LysoTracker Red and by indirect immunofluorescence staining with an antibody raised against LAMP1. The presence of acid vacuoles linked to the fusion of lysosomes and autophagic vacuoles was evaluated after staining with monodansylcadaverine (MDC). Data shown are representative from minimum three independent experiments.

Figure 4: Effects of VLCFA (C24:0 and C26:0) on autophagic process on 158N murine oligodendrocytes. A: Autophagy was evaluated in western blotting by conversion of LC3-I to LC3-II [ratio LC3-II/LC3-I], B: autophagic flux by the use of bafilomycin and in immunofluorescence staining with an antibody raised against p62 (C). D: The effect on cell growth, cell adhesion, and cell detachment was determined by phase contrast microscopy. Murine oligodendrocytes were cultured with C24:0 and C26:0 at 20 µM in presence or not of rapamycine at 5 µM for 24 and 48 h. The effects of VLCFA and/or rapamycin on cell proliferation and mitochondrial metabolism were evaluated with the MTT assay. Data shown are representative from minimum three independent experiments.

Figure 5: Effects VLCFA (C24:0 and C26:0) on a mixed primary culture from mouse brain. Mixed primary culture, from mouse brain, was cultured for 6, 14, 24 and 48 h in the absence or presence C24:0 and C26:0 at 10 and 20 µM. A: the effects of VLCFA on cell proliferation and mitochondrial metabolism were evaluated with the MTT assay. B: The integrity of cytoplasmic membranes of cells was evaluated with LDH assay. Data shown are mean ± SD from minimum three independent experiments realized in triplicat. Significance of the difference between VLCFA-treated cells and α-cyclodextrin-treated cells was determined with Mann-Whitney test: * $p < 0.05$; ** $p<0.01$, *** $p<0.001$, and # $p<0.0001$. C: Autophagy was evaluated in western blotting by conversion of LC3-I to LC3-II [ratio LC3-II/LC3-I], D: autophagic flux by the use of bafilomycin and E: in immunofluorescence staining with an antibody raised against p62.

Figure 6: Effects VLCFA (C24:0 and C26:0) on on X-ALD patient fibroblasts. Fibroblasts WT or X-ALD were cultured for 6, 14, 24 and 48 h in the absence or presence C24:0 and C26:0 at 10 and 20 µM. A: the effects of VLCFA on cell proliferation and mitochondrial metabolism were evaluated with the MTT assay. Data shown are mean ± SD from minimum three independent experiments realized in triplicat. Significance of the difference between VLCFA-treated cells and α-cyclodextrin-treated cells was determined with Mann-Whitney test: * $p < 0.05$; ** $p<0.01$, *** $p<0.001$, and # $p<0.0001$. B: Autophagy was evaluated in western blotting by conversion of LC3-I to LC3-II [ratio LC3-II/LC3-I], C: autophagic flux by the use of bafilomycin and D: in immunofluorescence staining with an antibody raised against p62.

Figure 7: Schematic representation of the the induction of cell death by VLCFA. The schema proposed is based on the data obtained in the present study. VLCFA first induce oxidative stress that impacts the mitochondrial activity. The exact relationship between mitochondria and peroxisome has yet to be defined. The induction of autophagy would make it possible to fight against mitochondrial and peroxisomal dysfunction and to eliminate altered mitochondria and peroxisomes. If the autophagic process is not sufficient to prevent cell death, the cells would move towards cell death.

Supplementary data 1: Evaluation of the apoptotic process on 158N cells. Nuclear condensation and/or fragmention characteristic of apoptotic cells was realized by staining with Hoechst 33342 (A); the evaluation of DNA fragmentation was determined by the TUNEL technic (B) and the cleavage of caspase-3 was determined by western blotting (C). 158N cells were treated with VLCFA at 10 and 20 µM for 24 h and 48 h, or with 7-ketocholesterol at 50 µM (7KC) for 24 h, used as a positive apoptotic control. A: 158N cells were incubated with Hoechst 33342 at 2 µg/mL and observed under a fluorescence microscope at x1000 magnification. B: The fragmented DNA was labelled by the TUNEL technique (green fluorescence) and the cell nuclei were stained with Hoechst 33342 at 2 µg/mL (blue fluorescence). C: The result presented for caspase 3 was obtained by western blot; it is representative of 3 experiments carried out independently; the ratio (density cleaved Caspase 3 / density uncleaved Caspase 3) was determined.

Supplementary data 2 : Evaluation of cytotoxicity of VLCFA (C24:0 and C26:0) in presence of 3 MA (3-methyladenin) on 158N murine oligodendrocytes. 158N cells were cultured for 24 h in the absence or presence C24:0 and C26:0 at 10 or 20 µM with or without 3-methyladenin at 7.5 mM. The effects of VLCFA on cell proliferation and mitochondrial metabolism were evaluated with the MTT assay. Significance of the difference between VLCFA-treated cells and VLCFA and 3MA-treated cells was determined with Mann-Whitney test: * $p < 0.05$; ** $p<0.01$, *** $p<0.001$, and # $p<0.0001$.

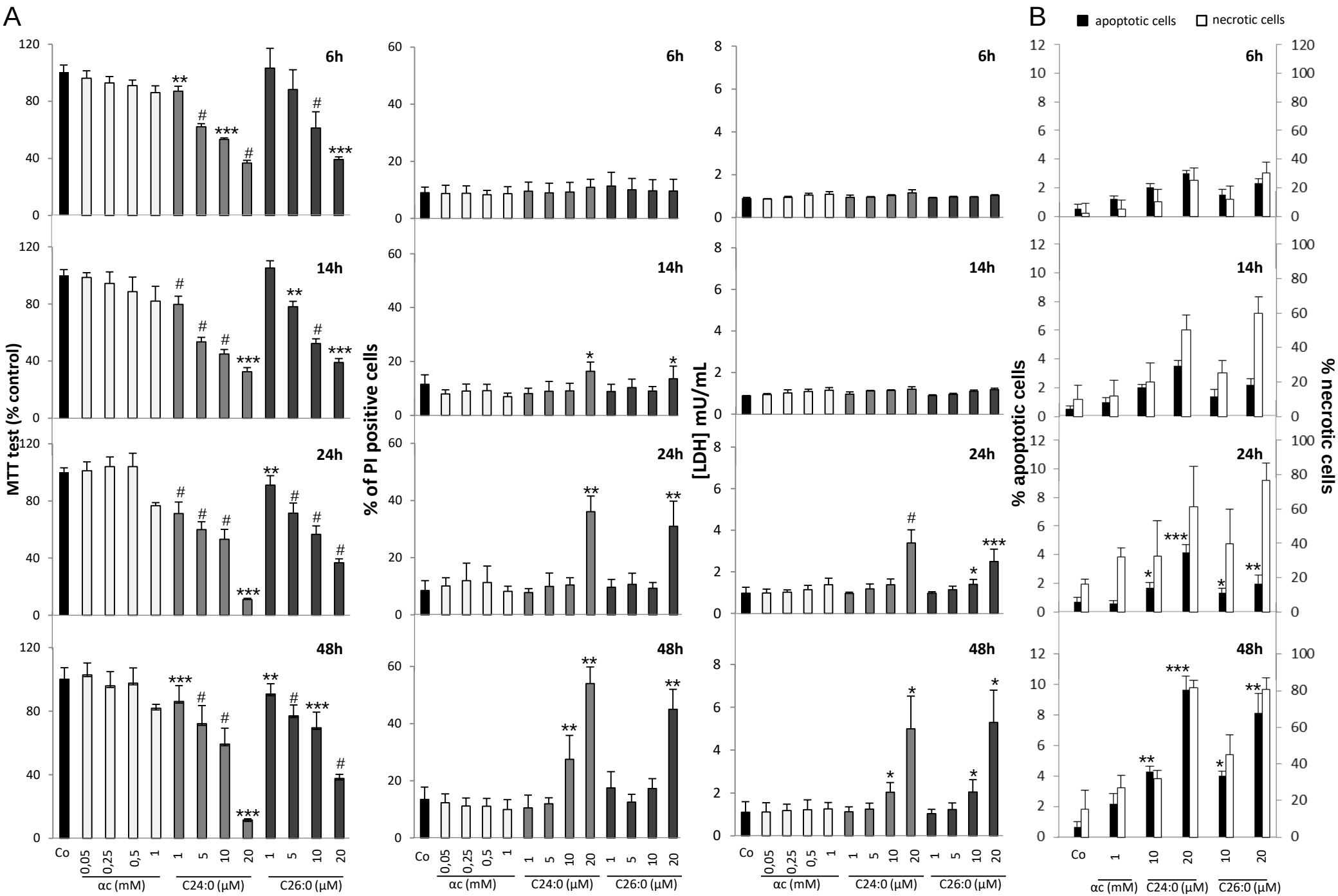
A
B
apoptotic cells
necrotic cells
MTT test (% control)
% of PI positive cells
[LDH] mU/mL
% apoptotic cells
% necrotic cells
6h
14h
24h
48h
Co
0,05
0,25
0,5
1
5
10
20
αc (mM)
C24:0 (μM)
C26:0 (μM)

Fig 1

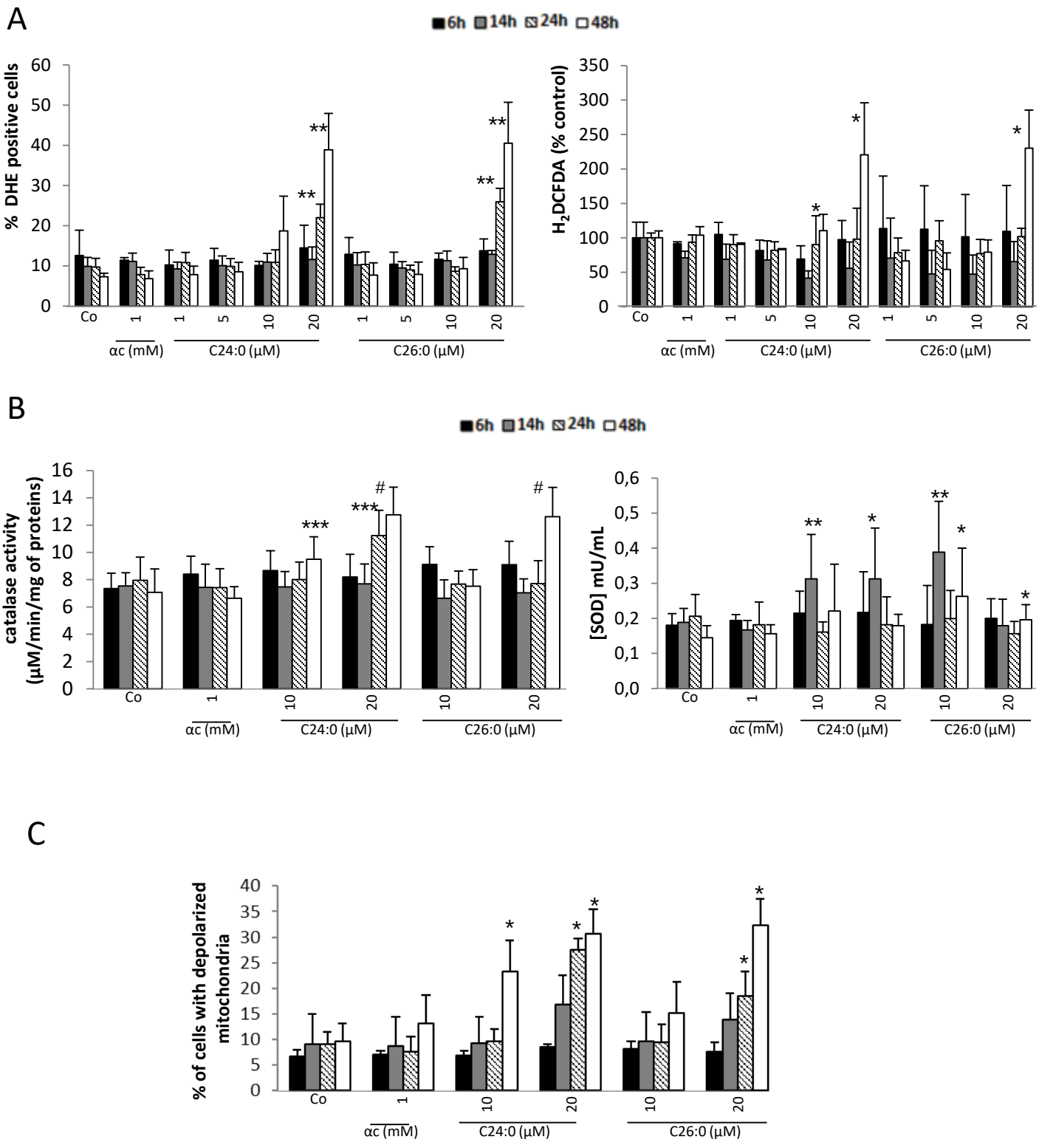
A
6h 14h 24h 48h
% DHE positive cells
H2DCFDA (% control)
Co
αc (mM)
C24:0 (μM)
C26:0 (μM)
B
6h 14h 24h 48h
catalase activity (μM/min/mg of proteins)
[SOD] mU/mL
C
% of cells with depolarized mitochondria

Fig 2

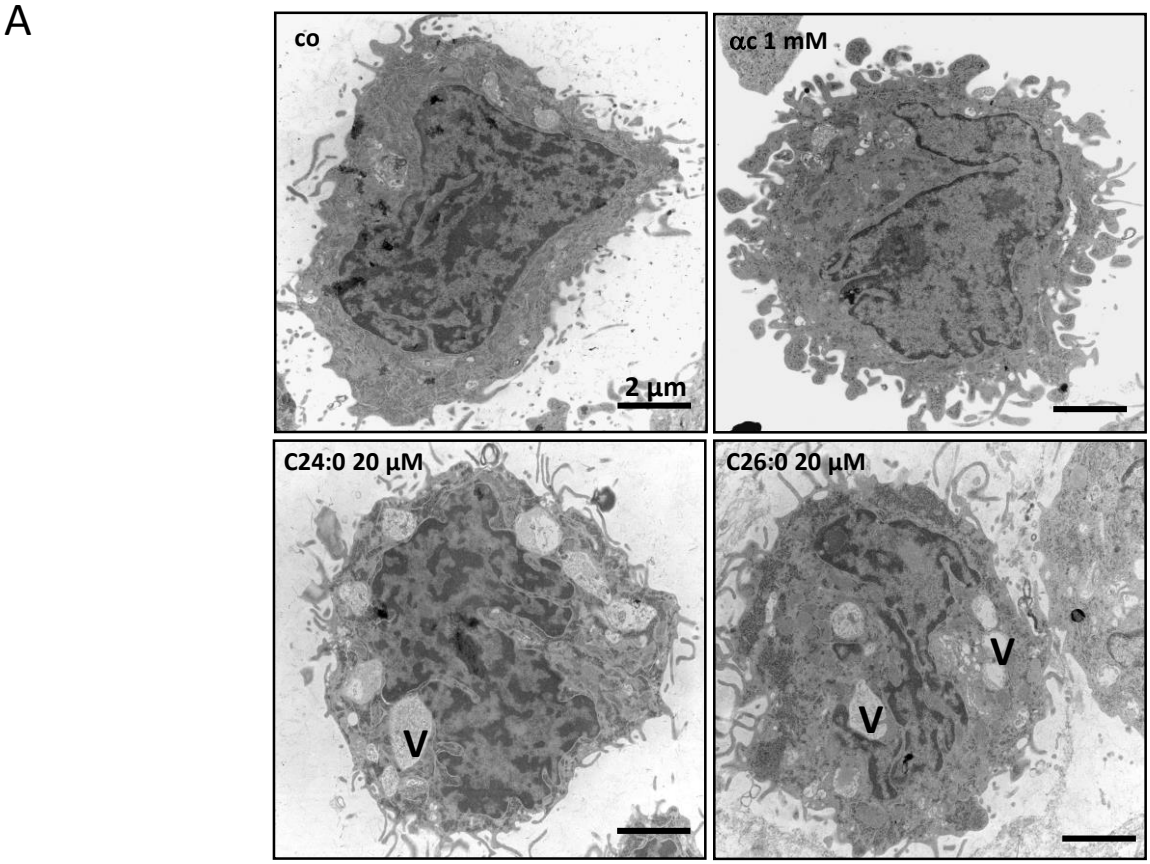
A
co
αc 1 mM
2 µm
C24:0 20 µM
C26:0 20 µM
V
V
V

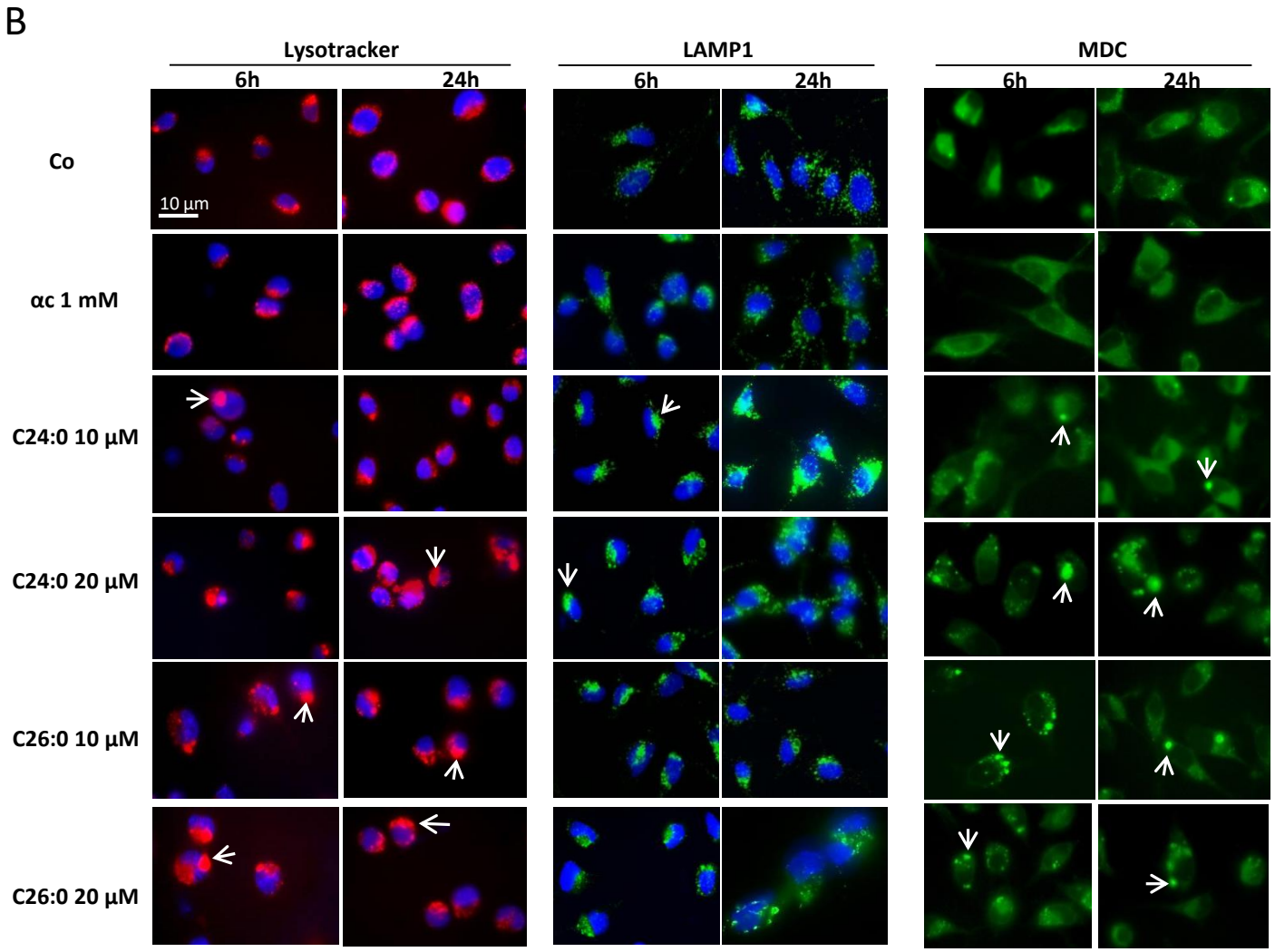
B
Lysotracker
LAMP1
MDC
6h
24h
6h
24h
6h
24h
Co
10 µm
αc 1 mM
C24:0 10 µM
C24:0 20 µM
C26:0 10 µM
C26:0 20 µM

Fig 3

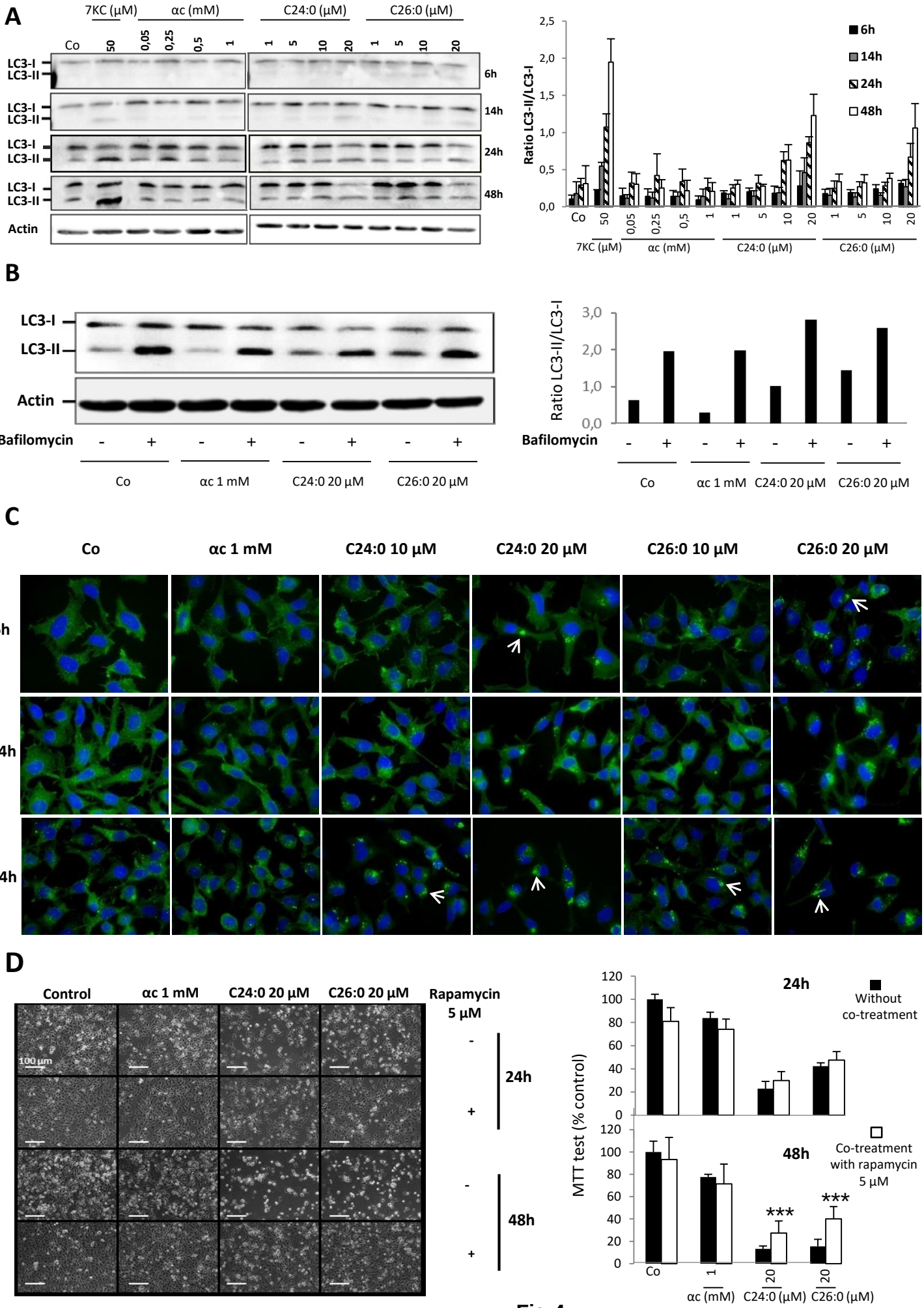
A
7KC (μM)
αc (mM)
C24:0 (μM)
C26:0 (μM)
Co
50
0,05
0,25
0,5
1
1
5
10
20
1
5
10
20
LC3-I
LC3-II
6h
14h
24h
48h
Actin
Ratio LC3-II/LC3-I
6h
14h
24h
48h
B
LC3-I
LC3-II
Actin
Bafilomycin
Co
αc 1 mM
C24:0 20 μM
C26:0 20 μM
C
Co
αc 1 mM
C24:0 10 μM
C24:0 20 μM
C26:0 10 μM
C26:0 20 μM
6h
14h
24h
D
Control
αc 1 mM
C24:0 20 μM
C26:0 20 μM
Rapamycin 5 μM
100 μm
24h
48h
MTT test (% control)
Without co-treatment
Co-treatment with rapamycin 5 μM
***
αc (mM)
C24:0 (μM)
C26:0 (μM)

Fig 4

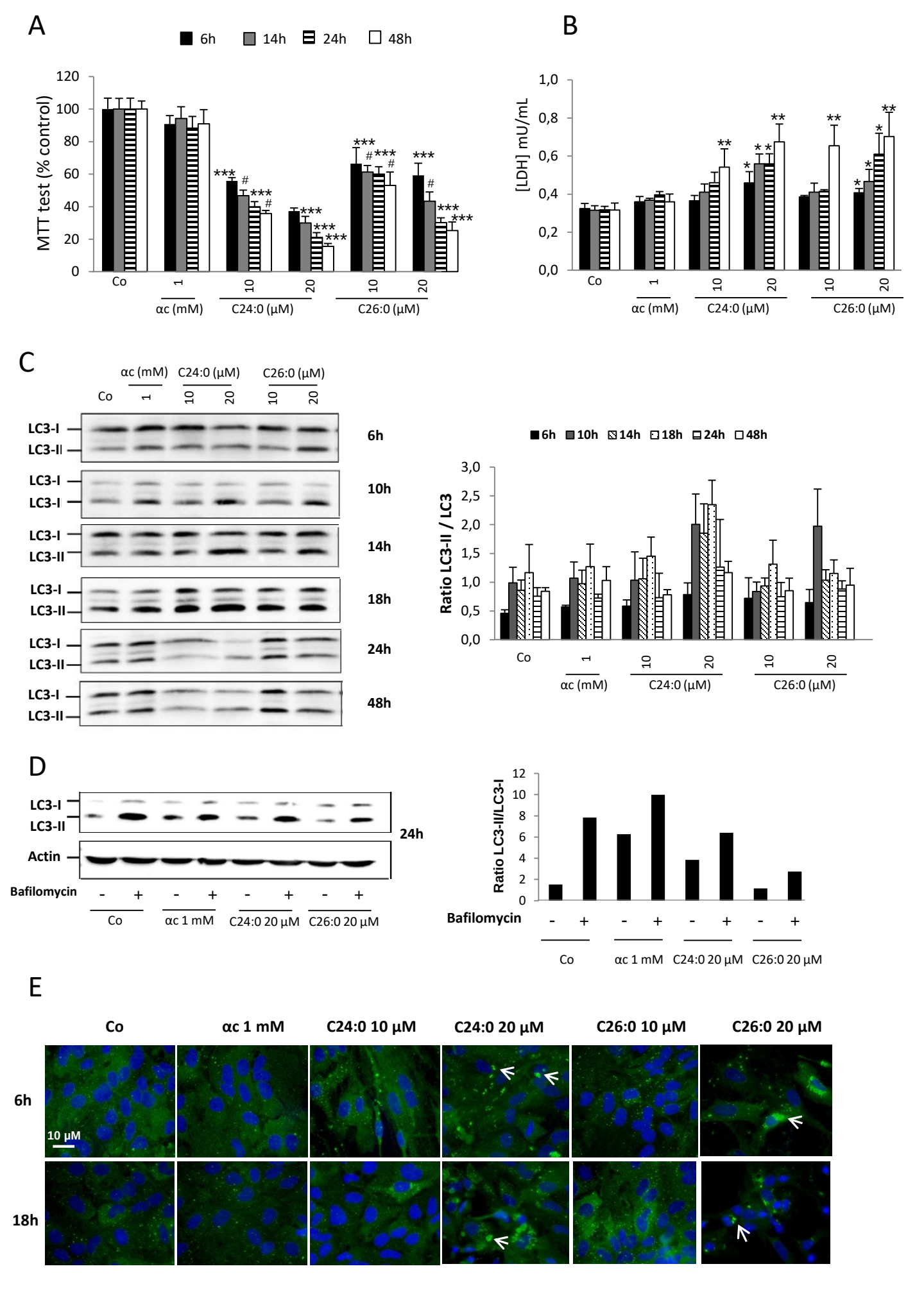
A
6h
14h
24h
48h
MTT test (% control)
Co
αc (mM)
C24:0 (μM)
C26:0 (μM)
B
[LDH] mU/mL
C
LC3-I
LC3-II
6h
10h
14h
18h
24h
48h
Ratio LC3-II / LC3
D
Actin
Bafilomycin
Co
αc 1 mM
C24:0 20 μM
C26:0 20 μM
Ratio LC3-II/LC3-I
E
Co
αc 1 mM
C24:0 10 μM
C24:0 20 μM
C26:0 10 μM
C26:0 20 μM
10 μM

Fig 5

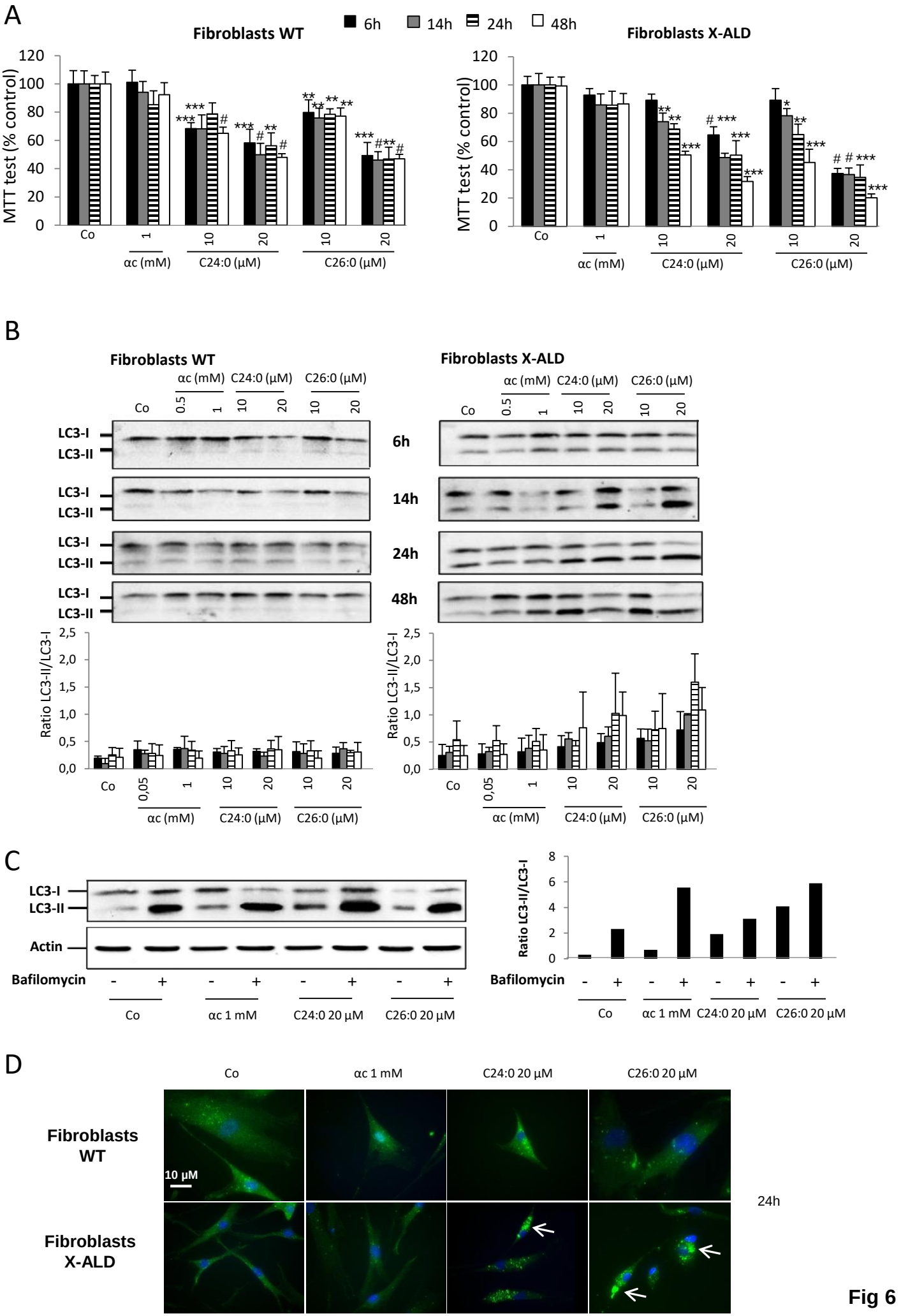
A
Fibroblasts WT
6h
14h
24h
48h
Fibroblasts X-ALD
MTT test (% control)
Co
αc (mM)
C24:0 (μM)
C26:0 (μM)
B
Fibroblasts WT
Fibroblasts X-ALD
LC3-I
LC3-II
6h
14h
24h
48h
Ratio LC3-II/LC3-I
C
Actin
Bafilomycin
Co
αc 1 mM
C24:0 20 μM
C26:0 20 μM
D
Fibroblasts WT
Fibroblasts X-ALD
10 μM
24h

Fig 6

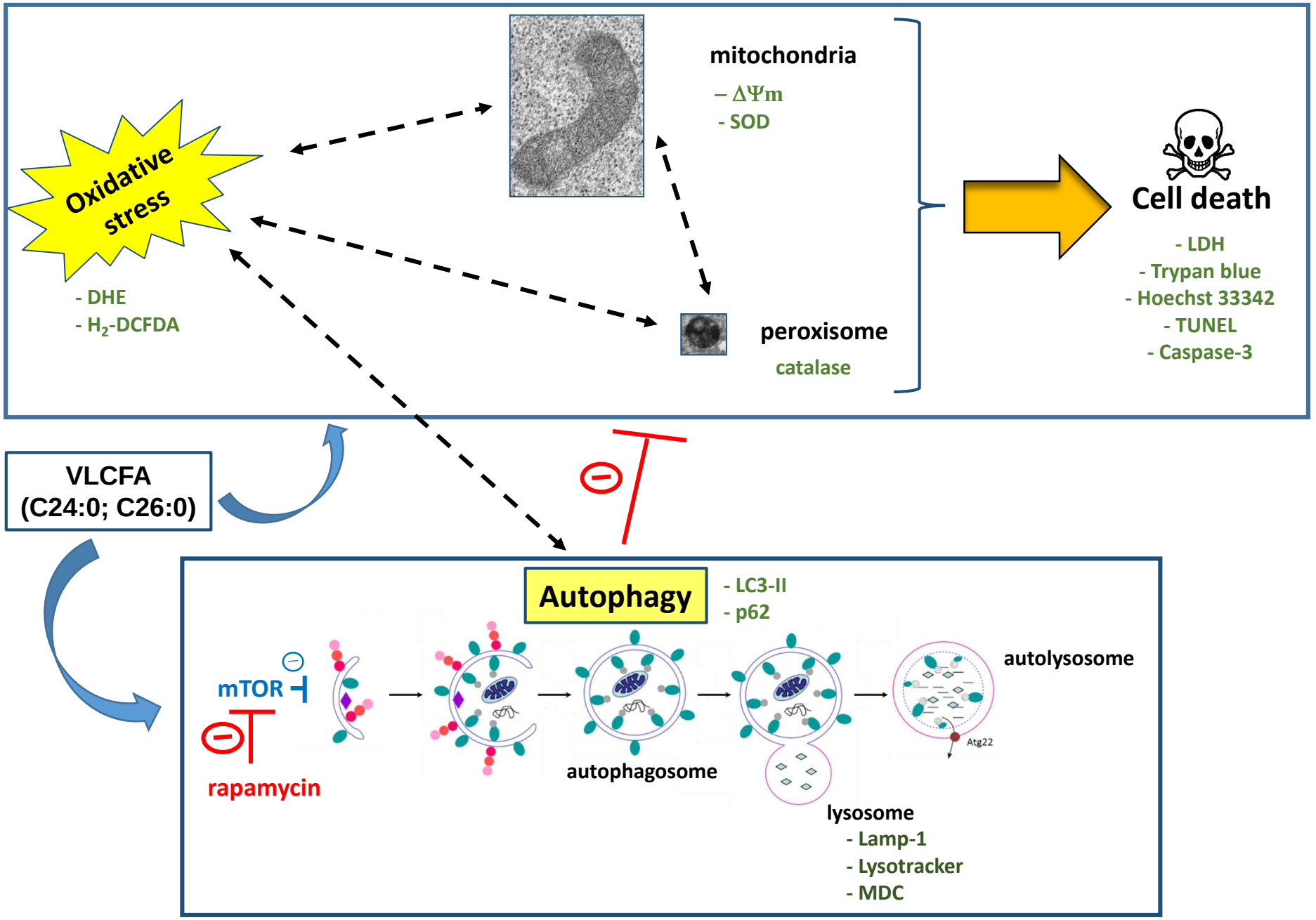
Oxidative stress
- DHE
- H2-DCFDA
mitochondria
– ΔΨm
- SOD
peroxisome
catalase
Cell death
- LDH
- Trypan blue
- Hoechst 33342
- TUNEL
- Caspase-3
VLCFA
(C24:0; C26:0)
Autophagy
- LC3-II
- p62
mTOR
rapamycin
autophagosome
lysosome
- Lamp-1
- Lysotracker
- MDC
autolysosome
Atg22
PI3K class III complex
LC3-II
Atg12-Atg5-Atg16
p62
proteins
mitochondria

Fig 7

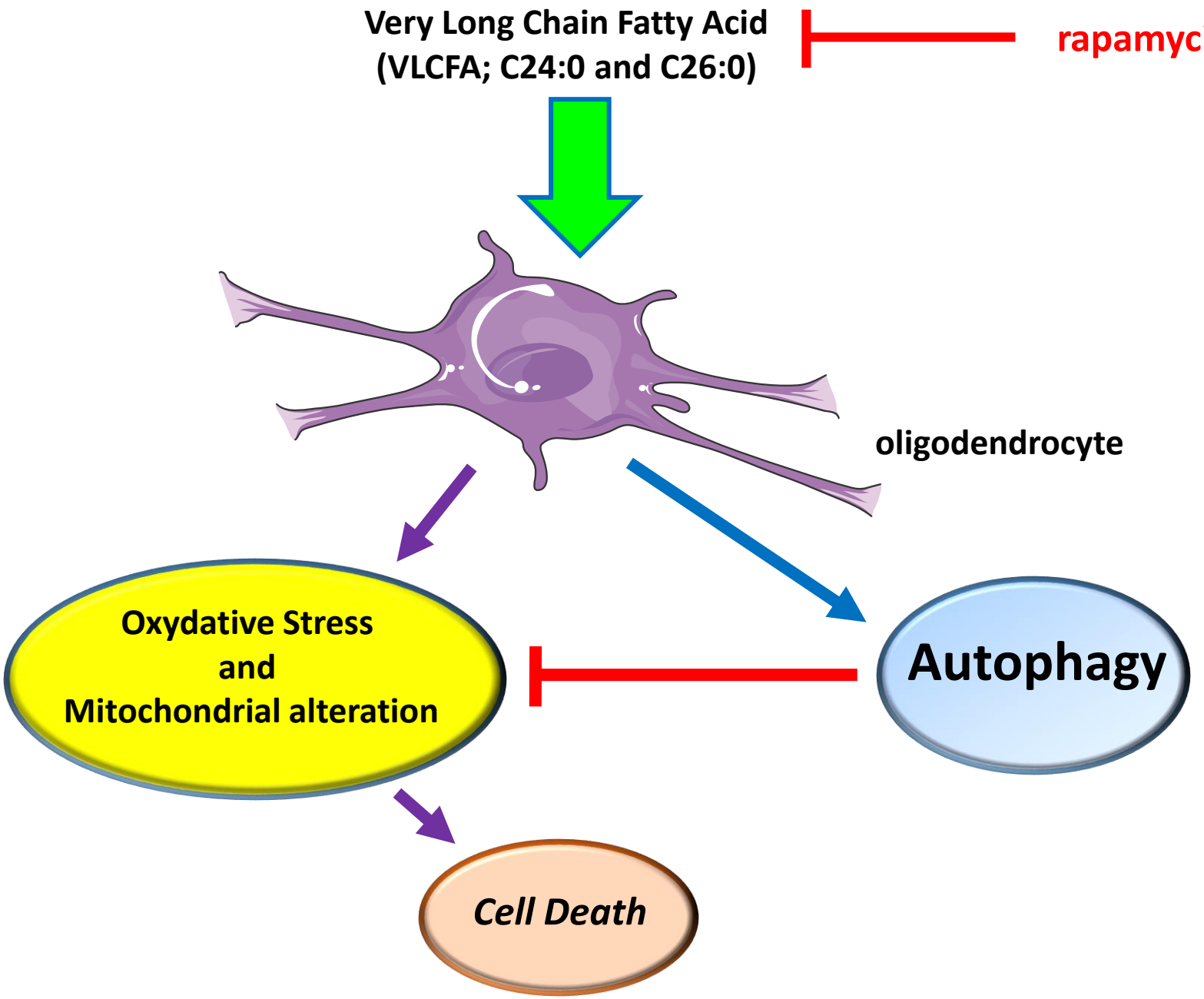

Graphical Abstract Doria et al.